Franck–Condon factors in curvilinear coordinates: the photoelectron spectrum of ammonia

Theor Chem Acc manuscript No.
(will be inserted by the editor)

Franck Condon factors in curvilinear coordinates: the photoelectron spectrum of ammonia

Amedeo Capobianco · Raffaele Borrelli · Canio Noce · Andrea Peluso

Received: date / Accepted: date

Abstract An approach to the calculation of Franck-Condon factors in curvilinear coordinates is outlined. The approach is based on Gribov's concept of curvilinear normal coordinates, which allows for an easy extension of Duschinsky's transformation to the case of curvilinear coordinates, and on the power series expansion of the kinetic energy operator. Its usefulness in the case of molecules undergoing large displacements of their equilibrium nuclear configurations upon excitation is then demonstrated by an application to the vibrational structure of the photoelectron spectrum of ammonia, whose equilibrium geometry is known to undergo a large shift upon photoionization, changing from pyramidal to planar.

Keywords Franck Condon factors · curvilinear coordinates · photoelectron spectra

Introduction

Ammonia is a very interesting molecule for spectroscopists and theoreticians. In the ground electronic state it exhibits two distinct equilibrium nuclear configurations which, by interconverting each other along the large amplitude motion, the so called umbrella motion, cause the splitting of the rovibrational energy levels. Furthermore, ammonia undergoes significantly large displacements of its equilibrium nuclear geometry upon excitation and photoionization, which reflect into broad absorption bands, with a well resolved vibrational and rovibrational structure, as shown in Fig. 1 for the $^2\mathrm{A}_1'' \leftarrow \tilde{\mathrm{X}}^1\mathrm{A}_1$ transition. The analyses of both the vibrational pattern [1] and of the rotational fine structure of some vibronic peaks [2] of the UV absorption band occurring at 217 nm have led to the conclusion that the excited electronic state has a planar equilibrium nuclear configuration, belonging to D_{3h} point group. A very similar vibrational pattern has also been observed in the lower energy region of its photoelectron spectrum, leading to the conclusion that even the $^2\mathrm{A}_1$ ionic state is planar [3–5].

Both the splitting of the energy levels of the rovibrational spectrum and the well resolved vibrational pattern of the electronic and photoelectronic spectra provide important experimental data for theoreticians involved in the application of sophisticated theoretical models for treating strong anharmonic effects [6,7], and in the development of efficient methodologies for the calculations of spectroscopic band shapes, *i.e.* Franck-Condon (FC) factors. It is indeed well known that in the case an electronic transition takes place between two electronic states exhibiting a large displacement of their equilibrium positions the calculation of the FC factors may pose problems, especially when the Cartesian representation of normal modes and the harmonic approximation are adopted [8,9]. In fact, in rectilinear coordinates a large displacement along a bending coordinate always implies a motion along the two bond distances forming the valence angle, Fig. 2, so that on carrying out the projection of the normal modes of one

A. Capobianco · C. Noce
Dipartimento di Fisica E.R. Caianaiello
Università di Salerno
Via Ponte don Melillo
I-84084 Fisciano (SA) Italy

R. Borrelli · A. Peluso
Dipartimento di Chimica e Biologia
Università di Salerno
Via Ponte don Melillo
I-84084 Fisciano (SA) Italy
E-mail: apeluso@unisa.it

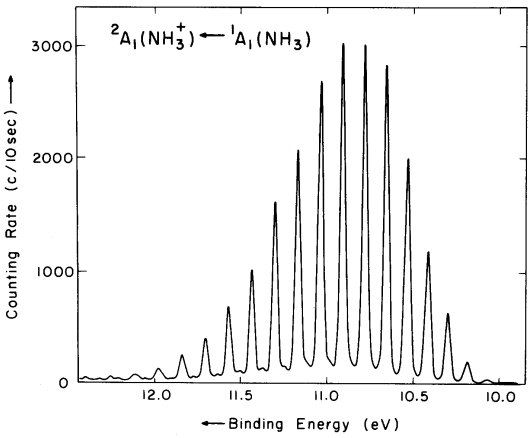

Fig. 1 The lowest energy band of the photoelectron spectrum of ammonia, reproduced with permission from Rabalais J.W. et al, (1973) J Chem Phys 58:3370

electronic state onto those of the other – the Duschinsky transformation – those stretching modes come out to be significantly displaced, causing the appearance in the computed spectrum of several vibrational progressions, due to excitations of both the large amplitude and the stretching modes, which have no counterparts in the observed spectrum [9,10].

The most successful attempts to rationalize the photoelectron spectrum of ammonia through the computation of Franck-Condon factors was based on procedures which overcome Duschinsky's transformation, avoiding the use of normal modes of both electronic states.[11–14] Recently, a satisfying reproduction of the photoelectron spectrum of ammonia, based on Duschinsky's transformation and the Cartesian representation of the normal coordinates, has been obtained. However, a high order polynomial, describing the strong anharmonic couplings between the symmetric stretching mode and the umbrella motion, was necessary for correcting the several progressions caused by the spurious displacement of the symmetric stretching mode predicted by Duschinsky transformation in the Cartesian representation of the normal modes [10]. The adopted methodology is therefore quite cumbersome, requiring the knowledge of the potential energy of NH_3^+ on a large grid of nuclear coordinates. In the present work, with the aim of setting up an easier and general procedure to compute the FC factors for floppy molecules, those undergoing large displacements of their equilibrium positions upon light excitation, we afford the computation of the ammonia photoelectron spectrum by using internal curvilinear coordinates, with the hope of relieving the high computational effort of computing anharmonic potential energy terms.

Theoretical Approach

Curvilinear internal coordinates such as bond elongations (stretching) or variations of valence angles (bending) are potentially the best suited to treat molecular vibrations. Fig. 2 gives the classical description of the bending motion for an AB_2 linear molecule [15], both in linearized internal coordinates (a) and in true curvilinear internal coordinates (b). In curvilinear coordinates nuclei are allowed to follow curved trajectories, whereas linearized internal coordinates force nuclear motion along straight lines, defined by the projections of the exact internal coordinates onto fixed Cartesian axes. A linearized internal coordinate s_j coincides with the curvilinear one S_j in the limit of infinitesimal displacements of atoms from their equilibrium positions. Therefore in the range of validity of the harmonic approximation there is no distinction between linear and curvilinear coordinates, but when large displacements are involved, such as those observed in going from the equilibrium geometry of NH_3 to that of NH_3^+, the two sets of coordinates are no longer equivalent. In the example of Fig. 2, the motion along a linearized bending coordinate involves an elongation of the A-B bond. Even if the potential energy were strictly quadratic in curvilinear coordinates, anharmonic terms would be needed in the rectilinear representation to obtain an equivalent description of the nuclear motion.[16] Of course, both the rectilinear and the curvilinear representation must lead to identical results when an exact treatment of the vibrational problem is carried out, but they yield different results at lower orders of approximation. In particular, the expression of the potential energy in curvilinear coordinates is generally simpler than that obtained by adopting rectilinear coordinates [15–17], but the linear momentum and the kinetic energy operators in curvilinear coordinates are much more involved [18–21].

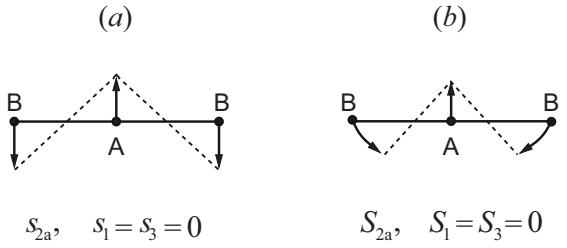

Fig. 2 Representations of the bending motion (at arbitrary low speed) in rectilinear (a) and curvilinear (b) coordinates for the linear molecule AB_2. S denotes curvilinear coordinates, s rectilinear ones.

The quantum vibrational Hamiltonian in curvilinear coordinate is [18]:

$$\hat{H}_S = -\frac{\hbar^2}{2} G^{1/4} \left(\frac{\partial}{\partial \mathbf{S}}\right)^T G^{-1/2}\, \mathbf{G} \left(\frac{\partial}{\partial \mathbf{S}}\right) G^{1/4} + V, \quad (1)$$

where $\mathbf{S}$ is the column vector of curvilinear internal coordinates, V is the potential energy, $\mathbf{G}$ and G are the metric matrix and its determinant, respectively, both depending on $\mathbf{S}$. The subscript S in the operator indicates normalization with respect to the $\mathbf{S}$ coordinates and the superscript T denotes transposition. By performing the differentiation, Eq. 1 can be rewritten as:

$$\hat{H}_S = -\frac{\hbar^2}{2} \sum_{j,k} \frac{\partial}{\partial S_j} G_{jk}(S) \frac{\partial}{\partial S_k} + V(S) + V_{\text{kin}}(S), \quad (2)$$

where

$$V_{\text{kin}} = \frac{5\hbar^2}{32G^2} \sum_{j,k} G_{jk} \frac{\partial G}{\partial S_j} \frac{\partial G}{\partial S_k} - \frac{\hbar^2}{8G} \sum_{j,k} \frac{\partial G_{jk}}{\partial S_j} \frac{\partial G}{\partial S_k} - \frac{\hbar^2}{8G} \sum_{j,k} G_{jk} \frac{\partial^2 G}{\partial S_j \partial S_k} \quad (3)$$

collects the terms of the kinetic energy operator which depend only on coordinates, thus acting like a potential energy term. The easiest way of taking properly into account the dependence of G_{jk} on $\mathbf{S}$ coordinates is that of expanding them into a power series. That yields:

$$\hat{H}_S = -\frac{\hbar^2}{2} \left(\sum_{j,k} G^0_{jk} \frac{\partial^2}{\partial S_j \partial S_k} + \sum_{j,k,\ell} G'_{jk\ell} \frac{\partial}{\partial S_j} S_\ell \frac{\partial}{\partial S_k} + \frac{1}{2} \sum_{j,k,\ell,m} G''_{jk\ell m} \frac{\partial}{\partial S_j} S_\ell S_m \frac{\partial}{\partial S_k} + \dots \right) + V_{\text{kin}} \quad (4)$$

where:

$$G^0_{jk} = G_{jk}(0) \quad (5)$$

$$G'_{jk\ell} = \left(\frac{\partial G_{jk}}{\partial S_\ell}\right)_0; \quad (6)$$

$$G''_{jk\ell m} = \left(\frac{\partial^2 G_{jk}}{\partial S_\ell \partial S_m}\right)_0. \quad (7)$$

The Hamiltonian in eq. 4 can be cast into a more manageable form by introducing curvilinear normal coordinates [18,22,23]. First, the so-called linearized internal coordinates, which are linear combinations of Cartesian displacements [24], are introduced:

$$\mathbf{s} = \mathbf{B}_0 \boldsymbol{\sigma}, \quad (8)$$

where $\mathbf{s}$ and $\boldsymbol{\sigma}$ are the column vectors of the linearized internal and the Cartesian displacement coordinates, respectively, and $\mathbf{B}_0$ is the Jacobian matrix whose elements depend only on the equilibrium geometry of the molecule. Normal coordinates $\mathbf{Q}$ are linear combinations of linearized internal coordinates:

$$\mathbf{s} = \mathbf{L}_0 \mathbf{Q}, \quad (9)$$

in which:

$$\mathbf{L}_0 = \frac{\partial \mathbf{s}}{\partial \mathbf{Q}} = \mathbf{B}_0 \mathbf{M}^{-1/2} \boldsymbol{\mathcal{L}}, \quad (10)$$

where $\mathbf{M}$ is the diagonal matrix of atomic masses and $\boldsymbol{\mathcal{L}}$ is the normalized matrix of normal modes in Cartesian coordinates, whose elements are not a function of the coordinates. The linear relationship between $\mathbf{Q}$ and $\mathbf{s}$ ensures that the elements of matrix of the effective masses:

$$\mathbf{G}^0 = \mathbf{L}_0 \mathbf{L}_0^T, \quad (11)$$

do not depend on the coordinates $\mathbf{s}$.

Then, "curvilinear normal coordinates" $\bar{\mathbf{Q}}$, defined as:

$$\mathbf{S} = \mathbf{L}_0 \bar{\mathbf{Q}}, \quad (12)$$

are introduced so that the vibrational Hamiltonian (2) assumes the form:

$$\hat{H} = -\frac{\hbar^2}{2} \sum_{r,s} \frac{\partial}{\partial \bar{Q}_r} g_{rs} \frac{\partial}{\partial \bar{Q}_s} + V(\bar{Q}) + V_{\text{kin}}(\bar{Q}), \quad (13)$$

where:

$$\mathbf{g} = \mathbf{R}^T \mathbf{G} \mathbf{R}; \quad \mathbf{R} = \left(\mathbf{L}_0^{-1}\right)^T. \quad (14)$$

In the limit of infinitesimal vibrational amplitudes, curvilinear internal coordinates coincide with linearized ones therefore (Eq.s 9 and 12) curvilinear normal coordinates coincide with the linear ones. This in turn implies that: *i)* $\mathbf{g}^0$, i.e. the metric matrix over curvilinear normal coordinates at the zero order of expansion, coincides with the unit matrix and *ii)* anharmonic terms vanish in the potential energy expressed as a function of $\bar{Q}$. A power series expansion provides a kinetic energy operator of the form:

$$\hat{T} = -\frac{\hbar^2}{2} \sum_r \frac{\partial^2}{\partial \bar{Q}_r^2} + \Delta\hat{T} + V_{\text{kin}}. \quad (15)$$

$\Delta\hat{T}$ and V_{kin} being the kinetic energy terms originated by the curvilinear nature of $\bar{Q}$:

$$\Delta\hat{T}\left(\bar{Q}, \frac{\partial}{\partial \bar{Q}}\right) = -\frac{\hbar^2}{2} \left(\sum_{r,s,t} g'_{rst} \frac{\partial}{\partial \bar{Q}_r} \bar{Q}_t \frac{\partial}{\partial \bar{Q}_s} + \frac{1}{2} \sum_{r,s,t,u} g''_{rstu} \frac{\partial}{\partial \bar{Q}_r} \bar{Q}_t \bar{Q}_u \frac{\partial}{\partial \bar{Q}_s} + \dots \right), \quad (16)$$

where, as before (eq. 6):[25]

$$g'_{rst} = \left(\frac{\partial g_{rs}}{\partial \bar{Q}_t}\right)_0 = \sum_{j,k,l} G'_{jk\ell} R_{jr} R_{ks} L^0_{\ell t}; \quad \text{etc.} \tag{17}$$

and a potential energy in the form:

$$V = 2\pi^2 c^2 \sum_r \tilde{\nu}_r^2 \bar{Q}_r^2 + \Delta V(\bar{Q}) \tag{18}$$

where ΔV collects the anharmonic terms of the potential and $\tilde{\nu}_r$ are the harmonic frequencies expressed as wavenumbers. Combining Eq.s 15 and 18, the vibrational Hamiltonian may be written as:

$$\hat{H} = \hat{H}_0 + \Delta\hat{T} + \Delta V + V_{\text{kin}}, \tag{19}$$

where and $\hat{H}_0$ is the harmonic Hamiltonian:

$$\hat{H}_0 = -\frac{\hbar^2}{2} \sum_r \frac{\partial}{\partial \bar{Q}_r^2} + 2\pi^2 c^2 \sum_r \tilde{\nu}_r^2 \bar{Q}_r^2; \tag{20}$$

Approximate eigenfunctions of $\hat{H}$ can be obtained by means of perturbation theory [26] or variational method, using the basis set of the eigenfunctions of $\hat{H}_0$.

$\bar{\mathbf{Q}}$ and $\mathbf{S}$ are linearly related by eq. (12), this is the key-point for the extension of Duschinsky's transformation [27] in curvilinear normal coordinates. Reminding that internal coordinates $\mathbf{S}$ represent displacements from equilibrium positions:

$$\mathbf{S} = \boldsymbol{\zeta} - \boldsymbol{\zeta}_0 = \mathbf{L}_0 \bar{\mathbf{Q}} \tag{21}$$

and denoting with a prime one of the electronic states involved in the transition:

$$\boldsymbol{\zeta} = \boldsymbol{\zeta}_0 + \mathbf{L}_0 \bar{\mathbf{Q}} \tag{22}$$

$$\boldsymbol{\zeta} = \boldsymbol{\zeta}'_0 + \mathbf{L}'_0 \bar{\mathbf{Q}}'. \tag{23}$$

By equating (22) and (23) and eliminating $\bar{\mathbf{Q}}$:

$$\begin{aligned} \bar{\mathbf{Q}} &= \mathbf{L}_0^{-1}\mathbf{L}'_0\bar{\mathbf{Q}}' + \mathbf{L}_0^{-1}\left(\boldsymbol{\zeta}'_0 - \boldsymbol{\zeta}_0\right) \\ &= \mathbf{J}\bar{\mathbf{Q}}' + \mathbf{K} \end{aligned} \tag{24}$$

Results

Several sets of internal coordinates for describing the vibrational motion of ammonia in both the neutral and the cationic $^2A_1$ state have been proposed [7,15,28–30]. We have adopted the set suggested by Hoy et al. [15] and developed by Handy and coworkers [7], which, although not orthogonal in the whole range of nuclear coordinates as that of ref. [30], offers the advantage that the elements of the $\mathbf{G}$ matrix are already tabulated. It consists of the three N-H stretching coordinates (r_1, r_2, r_3), the angle (β) that each N-H bond forms with the trisector, i.e. the axis forming the same angle with each bond vector, see Fig. 3, and any two of the three valence angles (α_i) obtained by projecting ammonia onto a plane perpendicular to the trisector. The adopted set of coordinate is shown in Fig. 3. Instead of

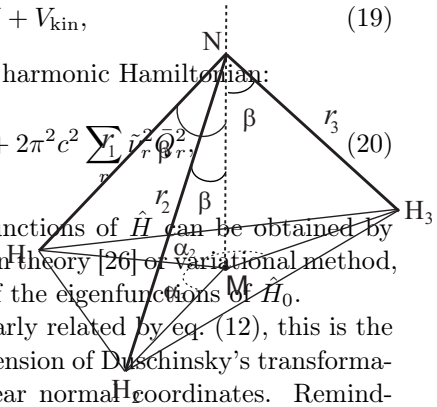

Fig. 3 Trisector axis (NM) at any nuclear configuration of ammonia: M belongs to the H_1-H_2-H_3 plane and is chosen in such a way that $\angle H_1NM = \angle H_2NM = \angle H_3NM = \beta$

r_1, r_2, r_3 we have used the symmetry adapted stretching coordinates R_1, R_2, R_3 defined as:

$$\begin{cases} R_1 = \dfrac{1}{\sqrt{3}}\left(r_1 + r_2 + r_3\right) \\ R_2 = \dfrac{1}{\sqrt{6}}\left(2r_1 - r_2 - r_3\right) \\ R_3 = \dfrac{1}{\sqrt{2}}\left(r_2 - r_3\right) \end{cases} \tag{25}$$

Harmonic vibrational frequencies and equilibrium geometries of the ground electronic states of NH_3 and NH_3^+, computed at fourth order of the Møller Plesset perturbation theory, including single, double and quadruple excitations, in conjunction with the 6-311++G(3df,3pd) basis set (hereafter MP4/TZ) are given in Table 1.

Table 1 Predicted[a] (MP4/TZ) bond lengths (r_{eq}, Å), valence angles (α_{eq}, degrees) and harmonic frequencies of the two symmetric mode ($\tilde{\nu}_i$ as wavenumbers, cm^{-1}) of NH_3 ($^1A_1$) and NH_3^+ ($^2A_1$).

	r_{eq}	α_{eq}	$\tilde{\nu}_1$[b]	$\tilde{\nu}_2$
$^1A_1$	1.0114	106.76	3523.94	1056.72
$^2A_1$	1.0203	120.00	3423.10	876.67

[a] From ref. [10]. [b] Herzberg notation, $\tilde{\nu}_{1(2)}$ refers to symmetric stretching(bending).

The $\mathbf{B}_0$ and $\mathbf{G}$ matrices have been evaluated following the procedure given in ref. [7] and transformed

according to Eq. (25). Analytical expressions of the elements of **G** are given in the Appendix. The coefficients g'_{rst} and g''_{rstu} appearing in the $\Delta\hat{T}$ term are reported in Table 2.

Table 2 First (u.m.a$^{-1/2}$Å^{-1}) and second order (u.m.a^{-1}Å^{-2}) power expansion non null coefficients of the kinetic energy of the ^{2}A$_1$ electronic state of cationic ammonia

g'_{212}	0.1217
g'_{221}	−1.1273
g''_{2222}	−0.1372
g''_{2211}	1.9063
g''_{1212}	−0.0686
g''_{1122}	0.1668

The potential energy surface of NH_3^+ as a function of $\bar{Q}_1$ and $\bar{Q}_2$, the symmetric stretching and bending curvilinear normal coordinates, respectively, has been calculated at the MP4/TZ level of approximation, over a grid of 431 points, covering the range $r_{\rm eq} - 0.05$ Å $\leq r \leq r_{\rm eq} + 0.05$ Å and $\alpha_{\rm eq} - 10^\circ \leq \alpha \leq \alpha_{\rm eq} + 10^\circ$. The potential energy has been fitted by different polynomials, one without coupling terms between the $\bar{Q}_1$ and the $\bar{Q}_2$ coordinates, the others with coupling terms having maximum order 4 in each variable. Since in the D_{3h} point group the totally symmetric stretching and the out of plane bending belong to different irreducible representations, all the terms in odd powers of $\bar{Q}_2$ are zero. The coefficients of the fitted polynomials are given in Table 3. It must be remarked that we have deliberately chosen to use a small grid of points, much smaller than that used previously in the literature [31, 10], in order to test the effectiveness of a good choice of internal curvilinear coordinates in relieving the computational efforts of computing anharmonic potential energy hypersurfaces for the calculation of FC factors.

Table 3 The coefficients of different polynomial fits of the potential energy surface of the $^2A_1$ electronic state of cationic ammonia in terms of curvilinear normal coordinates (coefficients in cm^{-1}/(amu$^{1/2}$ Å)^n, rms error in cm^{-1}).

	P1	P2	P3
q_2^2	11319.66	11319.66	11318.95
q_2^4	11885.66	11886.66	11799.86
q_1^2	173774.00	173774.00	173766.66
q_1^3	−279077.51	−206229.84	-206229.85
q_1^4	161562.75	161562.75	152225.84
$q_1q_2^2$		−14873.10	-14873.09
$q_1^2q_2^2$			3196.46
rms error	22.2	0.3	0.2

The photoelectron spectrum of ammonia consists of two transitions, one corresponding to the removal of an electron from the HOMO, the nitrogen lone pair $3a_1$ orbital, the $^2A_1'' \leftarrow \tilde{X}^1A_1$ transition, the other corresponding to the removal of an electron from the 1e orbital, the $^2E \leftarrow \tilde{X}^1A_1$ transition. The ground state electronic configuration is $1a_1^2 2a_1^2 1e^4 3a_1^2$ [4]. The $^2A_1'' \leftarrow \tilde{X}^1A_1$ lowest energy absorption exhibits a long vibrational progression, extending over about 2 eV and consisting of sixteen well resolved vibrational peaks see Fig. 1.[5] The highest intensities occur for the 7-th and 8-th peak, whose intensity are nearly the same,[5,32] but the origin of the band at lowest energy is still uncertain, it could be either the $0' \leftarrow 0$ transition or a hot band. The observed vibrational spacings is *ca.* 0.12 eV (970 cm^{-1}), so that the long vibrational progression has been assigned to the ν_2 mode (Herzberg's notation [33]), the so called umbrella mode. In the high resolution spectrum recorded by Edvardsson et al. [32], the strong progression due to the symmetric bending mode is accompanied by a much weaker but well resolved one, falling at higher energy, which was tentatively assigned to the asymmetric bending mode with one more quantum on the symmetric bending mode Q'_2.

As concerns neutral ammonia, a good representation of the two quasi-degenerate vibrational states is all we need for computing the photoelectron spectrum. A few test computations, carried out with an analytical anharmonic potential which reproduces the height of the inversion barrier (1882 cm^{-1}), showed that the lowest energy states are well described by the symmetric and antisymmetric linear combinations of the two lowest energy vibrational states of each nuclear configuration, no significant contributions of higher energy harmonic wavefunctions have been found. From the symmetric vibrational ground state, transitions to vibrational states with even quantum numbers are allowed, whereas states with odd quantum numbers are excited from the antisymmetric combination. Since the symmetric and antisymmetric vibrational modes of neutral ammonia are separated by only 0.79 cm^{-1} [29], Boltzmann populations of the two levels are equal and that allows to compute FC factors using only one equilibrium configuration of neutral ammonia. The initial state in all the FC calculations is therefore the harmonic ground vibrational state of the neutral molecule, the only one significantly populated at room temperature.

Among the six normal modes of the $^2A_1$ cationic state, only the symmetric stretching and the symmetric bending inversion modes, play a role in the photoelectron spectrum if vibronic couplings are neglected [32,10]. The stronger progression observed in the pho-

toelectronic spectrum extends over an energy range of about 2 eV, so that a good representation of at least the lowest sixteen states associated to the inversion mode is needed. Thus both potential anharmonic terms and the $\Delta\hat{T}$ kinetic terms are in principle important for this electronic state. Anharmonic wavefunctions of NH_3^+ have been computed by using the variational method, truncating the expansion of Eq. (16) to second order and neglecting the $V_{\rm kin}$ term, which is known to give very small contributions to the energies of the vibrational states [17,18]. Forty harmonic oscillator basis functions for each mode centered in the minimum energy nuclear configuration of the cationic state have been used; that choice ensures convergence on the excited vibrational states in an energy region much larger than that of interest. Eigenstates have been computed by an implicitly restarted Arnoldi procedure. Analytical integrals have been used.[34]

The $^2A_1'' \leftarrow \tilde{X}^1A_1$ photoelectronic spectrum of ammonia computed by considering a harmonic potential obtained at MP4/TZV level of computation, and the kinetic energy operator $\Delta\hat{T}$ of Eq. 16 is shown in figure 4.

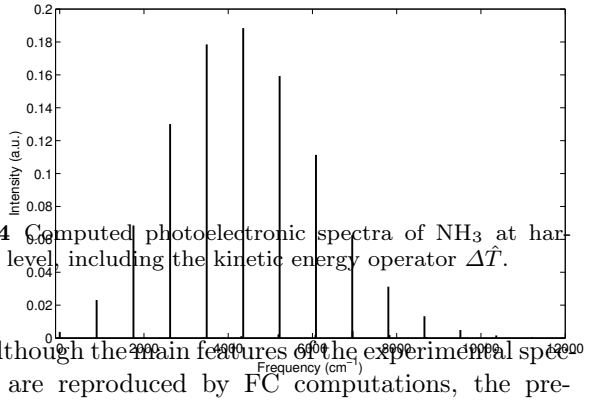

Fig. 4 Computed photoelectronic spectra of NH_3 at harmonic level, including the kinetic energy operator $\Delta\hat{T}$.

Although the main features of the experimental spectrum are reproduced by FC computations, the predicted intensity distribution is significantly different from the observed one. The maximum peak height occurs for the $5 \leftarrow 0$ transition, but the $6 \leftarrow 0$ one exhibits a significantly lower intensity than the $5 \leftarrow 0$ transition. More important discrepancies are observed in the high wavenumber region, where the relative intensities of the computed spectrum decay much faster than the experimental ones. The intensities of the higher-energy transitions are significantly underestimated, and therefore the spectrum exhibits only 13 peaks, whereas in the experimental one at least 16 peaks are clearly observed. The results obtained by using a harmonic potential are thus in many aspects similar to those previously obtained by employing the internal coordinate representation but using a simplified expression of $\hat{T}$, without including the $\Delta\hat{T}$ terms [35,10]. Indeed, the $\Delta\hat{T}$ kinetic operator only provides corrections of a few tens of cm^{-1} on the computed energies, without significantly affecting the computed eigenvectors.

The computed spectrum obtained by using the P_1 anharmonic potential of Table 3 together with kinetic $\Delta\hat{T}$ is shown in figure 5 and compared with the experimental intensities of ref. [32]. The latter ones have been obtained from the peak areas of the deconvoluted photoelectron spectrum. The whole spectrum is well reproduced, especially as concerns its decay in the longer wavenumber region, which had posed problems in previous theoretical investigations [12]. The experimental bandwidth is also well reproduced by FC calculations; Rabelais' experimental spectrum shows sixteen well resolved peaks, with a little not resolved tail, whereas the theoretical one exhibits one more. The computed spectrum also shows the presence of a second much weaker progression, which the calculation assigns to transitions to vibrational states with excitations on the bending mode Q_2' and a single quantum on the totally symmetric stretching mode Q_1', in agreement with previous theoretical results [13,14,10]. The weaker progression is very well resolved in the high resolution spectrum of Edvardsson et al,[32] who tentatively assigned it to transitions to a vibrational progression of the asymmetric bending mode with one more quantum on the symmetric bending mode Q_2'. The first mode is of E symmetry, and therefore vibronic couplings should be invoked to justify the presence of such combination bands in the experimental spectrum. In the experimental spectrum the weak progression starts just after the sixth peak of the stronger progression, about 5400 cm^{-1} after the $0' \leftarrow 0$ transition and exhibits a maximum for the third peak. In the computed spectrum the weak progression starts after the fifth peak and the maximum peak height falls at the forth peak. The adopted scaling was the same as for the main progression, thus the good agreement between the relative intensities of the weak and the strong progression further supports our assignment.

The computed spectra obtained by using the other potential energy functions of Table 3 are very similar to that obtained by using the simplest P1 potential as concerns the stronger progression; a slight detriment on the intensities and width of the weaker progression is observed when couplings between the Q_1' and Q_2' are introduced in the potential energy expressions, possibly because of the small grid used in the electronic calculations, not sufficiently large, especially for the totally

symmetric stretching mode, for providing the coupling terms with the required accuracy for calculations of the FC factors.

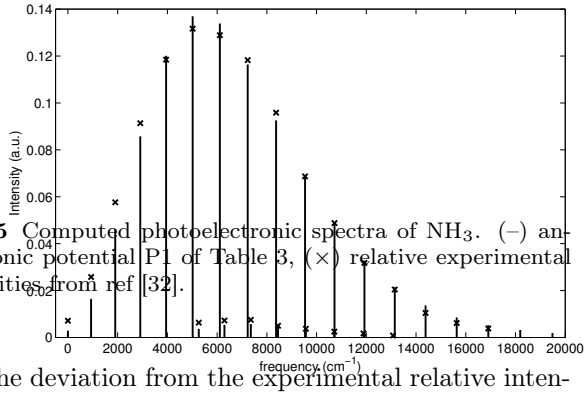

Fig. 5 Computed photoelectronic spectra of NH_3. (–) anharmonic potential P1 of Table 3, (×) relative experimental intensities from ref [32].

The deviation from the experimental relative intensities is more pronounced for low energy levels, whereas the high region of the spectrum is better reproduced. That unexpected behavior, the quality of the computed states should be higher than those at higher energy, can be due to the presence of overlapping bands in the experimental spectrum which makes it difficult the estimate of FC factors by the deconvolution technique. Indeed, on the assumption that the first observed band is a hot band, as experimental and theoretical evidence leads to suppose [32,13], a possible explanation of the low intensity is that other peaks of the hot progression could be hidden under the lower energy peaks. Indeed previous calculations of FC factors from the $|0\,1\rangle$ state of neutral ammonia indicates that the transition $0'\,0' \leftarrow 0\,1$ is not the most intense one, but it should be accompanied by at least four transitions of the type $n'\,0' \leftarrow 0\,1$ (n=1,2,$\cdots$) , which have still higher intensities.[10] Those hot transitions could affect the intensities of the peaks of the main progression making the comparison of the computed and the observed spectrum even more difficult.

Conclusion

Prediction of the band shapes for radiative transitions between electronic states with significantly different minimum energy nuclear configurations along an angular coordinate (floppy molecules) requires caution. Gribov's definition of curvilinear normal coordinates allows the generalization of Duschinsky's transformation to the case of curvilinear coordinates. Those coordinates can be extremely useful for floppy molecules, inasmuch they could allow for decoupling the displaced modes, making it easier the computation of the potential energy hypersurface. Here we have shown that the photoelectron spectrum of ammonia, the prototype of a floppy molecule, can be reproduced with sufficient accuracy by using the curvilinear internal coordinate representation of the normal modes of the neutral and ionic state, providing that anharmonic potential energy terms are properly included. However, the computational effort for the characterization of anharmonic potential energy terms is significantly relieved by using curvilinear coordinates, both because in the case of ammonia curvilinear coordinates allows for decoupling the two active modes with a good accuracy, and because of the limited number of electronic computations to be carried out for the characterization of the potential energy hypersurface. Indeed in the Cartesian coordinate representation a grid of about 4300 points, covering the range $0.57 \leq r \leq 1.65$ Å and $40^\circ \leq \alpha \leq 120^\circ$ was necessary for obtaining reasonable results, whereas in the present work a much smaller grid of 431 points, covering the range $r_{\rm eq} - 0.05$ Å $\leq r \leq r_{\rm eq} + 0.05$ Å and $\alpha_{\rm eq} - 10^\circ \leq \alpha \leq \alpha_{\rm eq} + 10^\circ$ has been sufficient. In the case of ammonia, probably because of the good choice of internal coordinates, the dependence of the G matrix terms upon the curvilinear coordinates play a minor role, it can be neglected if a high accuracy on frequencies is not required.

Computational details

MP4 and Franck-Condon factor computations were carried out by using the Gaussian 09 suite of programs [36] and a development version of the MolFC package [37–39].

Acknowledgements The financial support of the University of Salerno is gratefully acknowledged.

Appendix 1: The G matrix

In the following:

$$\alpha_1 = 2\,\pi - \alpha_2 - \alpha_3; \tag{26}$$

$$\psi_i = \frac{\alpha_i}{2}; \quad i = 1,\, 2,\, 3; \tag{27}$$

$$\mu = \frac{m_{\rm N}\, m_{\rm H}}{m_{\rm N} + m_{\rm H}}. \tag{28}$$

$$G_{\beta\beta} = \frac{\cos^2\psi_1}{4\mu\,\left(\sin^2\psi_2\right)\left(\sin^2\psi_3\right)\left(\frac{R_1}{\sqrt{3}}+\frac{2R_2}{\sqrt{6}}\right)^2}$$
$$+\frac{\cos^2\psi_2}{4\mu\left(\sin^2\psi_1\right)\left(\sin^2\psi_3\right)\left(\frac{R_1}{\sqrt{3}}-\frac{R_2}{\sqrt{6}}+\frac{R_3}{\sqrt{2}}\right)^2}$$
$$+\frac{\cos^2\psi_3}{4\mu\left(\sin^2\psi_1\right)\left(\sin^2\psi_2\right)\left(\frac{R_2}{\sqrt{6}}-\frac{R_1}{\sqrt{3}}+\frac{R_3}{\sqrt{2}}\right)^2}$$
$$+\frac{(\cot\psi_2)\,(\cot\psi_3)\left[2\left(\sin^2\psi_1\right)\left(\cos^2\beta\right)-1\right]}{2m_{\mathrm{N}}\left(\sin^2\psi_1\right)\left(\frac{R_2}{\sqrt{6}}-\frac{R_1}{\sqrt{3}}+\frac{R_3}{\sqrt{2}}\right)\left(\frac{R_1}{\sqrt{3}}-\frac{R_2}{\sqrt{6}}+\frac{R_3}{\sqrt{2}}\right)}$$
$$+\frac{(\cot\psi_1)\,(\cot\psi_2)\left[2\left(\sin^2\psi_3\right)\left(\cos^2\beta\right)-1\right]}{2m_{\mathrm{N}}\left(\sin^2\psi_3\right)\left(\frac{R_1}{\sqrt{3}}+\frac{2R_2}{\sqrt{6}}\right)\left(\frac{R_2}{\sqrt{6}}-\frac{R_1}{\sqrt{3}}-\frac{R_3}{\sqrt{2}}\right)}$$
$$+\frac{(\cot\psi_1)\,(\cot\psi_3)\left[2\left(\sin^2\psi_2\right)\left(\cos^2\beta\right)-1\right]}{2m_{\mathrm{N}}\left(\sin^2\psi_2\right)\left(\frac{R_1}{\sqrt{3}}+\frac{2R_2}{\sqrt{6}}\right)\left(\frac{R_2}{\sqrt{6}}-\frac{R_1}{\sqrt{3}}+\frac{R_3}{\sqrt{2}}\right)} \quad (29)$$

$$G_{R_1R_1} = \frac{1}{\mu} - \frac{4\sin^2\beta\left(\sin^2\psi_1+\sin^2\psi_2+\sin^2\psi_3\right)-6}{3m_{\mathrm{N}}} \quad (30)$$

$$G_{\beta R_1} = \frac{\sqrt{3}\sin(2\beta)}{6\,m_{\mathrm{N}}\sin\psi_2}\left(\frac{\cos\psi_3\sin\psi_1}{\frac{R_2}{\sqrt{6}}-\frac{R_1}{\sqrt{3}}+\frac{R_3}{\sqrt{2}}}-\frac{\cos\psi_1\sin\psi_3}{\frac{R_1}{\sqrt{3}}+\frac{2R_2}{\sqrt{6}}}\right)$$
$$-\frac{\sqrt{3}\sin(2\beta)}{6\,m_{\mathrm{N}}\sin\psi_3}\left(\frac{\cos\psi_1\sin\psi_2}{\frac{R_1}{\sqrt{3}}+\frac{2R_2}{\sqrt{6}}}+\frac{\cos\psi_2\sin\psi_1}{\frac{R_1}{\sqrt{3}}-\frac{R_2}{\sqrt{6}}+\frac{R_3}{\sqrt{2}}}\right)$$
$$-\frac{\sqrt{3}\sin(2\beta)}{6\,m_{\mathrm{N}}\sin\psi_1}\left(\frac{\cos\psi_2\sin\psi_3}{\frac{R_1}{\sqrt{3}}-\frac{R_2}{\sqrt{6}}+\frac{R_3}{\sqrt{2}}}-\frac{\cos\psi_3\sin\psi_2}{\frac{R_2}{\sqrt{6}}-\frac{R_1}{\sqrt{3}}+\frac{R_3}{\sqrt{2}}}\right) \quad (31)$$

References

1. A.D. Walsh, P.A. Warsop, Trans. Faraday Soc. **57**, 345 (1961)
2. A.E. Douglas, Discuss. Faraday Soc. **35**, 158 (1963)
3. G.R. Branton, D.C. Frost, F.G. Herring, C.A. McDowell, L.A. Stenhouse, Chem. Phys. Lett. **3**, 581 (1969)
4. M.J. Weiss, G.M. Lawrence, J. Chem. Phys. **53**, 214 (1970)
5. J.W. Rabalais, L. Karlsson, L.O. Werme, T. Bergmark, K. Siegbahn, J. Chem. Phys. **58**, 3370 (1973)
6. C. Leonard, N.C. Handy, S. Carter, J.M. Bowman, Spectrochim. Acta A **58**, 825 (2002)
7. N.C. Handy, S. Carter, S.M. Colwell, Mol. Phys. **96**, 477 (1999)
8. J.R. Reimers, J. Chem. Phys. **115**, 9103 (2001)
9. R. Borrelli, A. Peluso, J. Chem. Phys. **125**, 194308 (2006)
10. A. Peluso, R. Borrelli, A. Capobianco, J. Phys. Chem. A **113**, 14831 (2009)
11. W. Domcke, L.S. Cederbaum, H. Köppel, W. Von Niessen, Mol. Phys. **34**, 1759 (1977)
12. H. Ågren, I. Reineck, H. Veenhuizen, R. Maripuu, R. Arneberg, L. Karlsson, Mol. Phys. **45**, 477 (1982)
13. A. Viel, W. Eisfeld, S. Neumann, W. Domcke, U. Manthe, J. Chem. Phys. **124**, 214306 (2006)
14. A. Viel, W. Eisfeld, C.R. Evenhuis, U. Manthe, Chem. Phys. **347**, 331 (2008)
15. A.R. Hoy, I.M. Mills, G. Strey, Mol. Phys. **24**, 1265 (1972)
16. K. Kuchitsu, Y. Morino, Bull. Chem. Soc. Japan **38**, 805 (1965)
17. E.L. Sibert, J.T. Hynes, W.P. Reinhardt, J. Phys. Chem. **87**, 2032 (1983)
18. L.A. Gribov, W. Orville-Thomas, *Theory and Methods of Calculation of Molecular Spectra* (Wiley, Chichester, 1988)
19. L.A. Gribov, J. Struct. Chem. *(Engl. Transl.)* **33**, 478 (1992)
20. P. Villaseñor-González, J. Cisneros-Parra, Am. J. Phys. **49**, 754 (1981)
21. A. Nauts, X. Chapuisat, Mol. Phys. **55**, 1287 (1985)
22. L.A. Gribov, Opt. Spectrosc. **30**, 1247 (1970)
23. A.I. Pavlyuchko, L.A. Gribov, Opt. Spectrosc. **54**, 644 (1983)
24. E.B.J. Wilson, J.C. Decius, P.C. Cross, *Molcular Vibrations* (McGraw Hill, New York, 1955)
25. A.D. Isaacson, J. Phys. Chem. A **110**, 379 (2006)
26. C.R. Quade, J. Chem. Phys. **64**, 2783 (1976). See also erratum *ibid.* **79**, 4089 (1983)
27. F. Dushinsky, Acta Physicochim. URSS **7**, 551 (1937)
28. V. Špirko, J. Mol. Spectrosc. **101**, 30 (1983)
29. V. Špirko, W.P. Kraemer, J. Mol. Spectrosc. **133**, 331 (1989)
30. M. Ragni, A. Lombardi, P.R. Pereira Barreto, A.C. Peixoto Bitencourt, J. Phys. Chem. A **113**, 15355 (2009)
31. S.N. Yurchenko, W. Thiel, M. Carvajal, P. Jensen, Chem. Phys. **346**, 146 (2008)
32. D. Edvardsson, P. Baltzer, L. Karlsson, B. Wannberg, D.M.P. Holland, D.A. Shaw, E.E. Rennie, J. Phys. B **32**, 2583 (1999)
33. G. Herzberg, *Infrared and Raman Spectra of Polyatomic Molecules* (Van Nostrand Co., Inc., Princeton, N. J., 1945)
34. S. Califano, *Vibrational States* (Wiley, New York, 1976)
35. W.R. Harshbarger, J. Chem. Phys. **53**, 903 (1970)
36. M.J. Frisch, G.W. Trucks, H.B. Schlegel, G.E. Scuseria, M.A. Robb, J.R. Cheeseman, G. Scalmani, V. Barone, B. Mennucci, G.A. Petersson, H. Nakatsuji, M. Caricato, X. Li, H.P. Hratchian, A.F. Izmaylov, J. Bloino, G. Zheng, J.L. Sonnenberg, M. Hada, M. Ehara, K. Toyota, R. Fukuda, J. Hasegawa, M. Ishida, T. Nakajima, Y. Honda, O. Kitao, H. Nakai, T. Vreven, J.A. Montgomery, Jr., J.E. Peralta, F. Ogliaro, M. Bearpark, J.J. Heyd, E. Brothers, K.N. Kudin, V.N. Staroverov, R. Kobayashi, J. Normand, K. Raghavachari, A. Rendell, J.C. Burant, S.S. Iyengar, J. Tomasi, M. Cossi, N. Rega, J.M. Millam, M. Klene, J.E. Knox, J.B. Cross, V. Bakken, C. Adamo, J. Jaramillo, R. Gomperts, R.E. Stratmann, O. Yazyev, A.J. Austin, R. Cammi, C. Pomelli, J.W. Ochterski, R.L. Martin, K. Morokuma, V.G. Zakrzewski, G.A. Voth, P. Salvador, J.J. Dannenberg, S. Dapprich, A.D. Daniels, Ö. Farkas, J.B. Foresman, J.V. Ortiz, J. Cioslowski, D.J. Fox. Gaussian 09 Revision A.02. Gaussian Inc. Wallingford CT 2009
37. A. Peluso, F. Santoro, G. Del Re, Int. J. Quantum Chem. **63**, 233 (1997)

38. R. Borrelli, A. Peluso, J. Chem. Phys. **119**, 8437 (2003)
39. R. Borrelli, A. Peluso. MolFC: A program for Franck-Condon integrals calculation. Package available online at `http://www.theochem.unisa.it`